water

MDPI

Article

Influence of Filter Tube of Pumping Well on Groundwater Drawdown during Deep Foundation Pit Dewatering

Xuehan Zhang [1,2], Xuwei Wang [1,2] and Yeshuang Xu [1,2,*]

[1] State Key Laboratory of Ocean Engineering, School of Naval Architecture, Ocean, and Civil Engineering, Shanghai Jiao Tong University, 800 Dong Chuan Road, Minhang District, Shanghai 200240, China; xhzhang2019@sjtu.edu.cn (X.Z.); 392538143@sjtu.edu.cn (X.W.)

[2] Shanghai Key Laboratory for Digital Maintenance of Buildings and Infrastructure, Department of Civil Engineering, Shanghai Jiao Tong University, Shanghai 200240, China

* Correspondence: xuyeshuang@sjtu.edu.cn; Tel.: +86-21-6402-7259

Abstract: The partial penetrating waterproof curtain combined with pumping wells is widely applied to deep foundation pit dewatering engineering. The filter tube of the pumping well plays a critical role on the environment effect that resulted from foundation pit dewatering. This paper investigated the impact of the filter tube on the groundwater drawdown outside the pit to provide a theoretical basis for the foundation pit dewatering design. Three patterns according to the relative position of the waterproof curtain and the filter tube, which are called wall-well patterns, namely the full-closed pattern, part-closed pattern, and none-closed pattern, have been analyzed. By taking a practice engineering case in Shanghai as an example, the relationship among the proportion of the filter tube length to the dewatering aquifer thickness, the buried depth difference of the wall-well, and the groundwater drawdown difference at both sides of the waterproof curtain are discussed by numerical simulation. The full-closed pattern is the optimal wall-well pattern on the ideal condition. The suggested and optimal values of the filter tube length to the dewatering aquifer thickness are 38.7% and 58.2%. The suggested and optimal values of the buried depth difference of the wall-well are −6.41 m and −1.92 m.

Keywords: filter tube; pumping well; groundwater drawdown; waterproof curtain; deep foundation pit dewatering

Citation: Zhang, X.; Wang, X.; Xu, Y. Influence of Filter Tube of Pumping Well on Groundwater Drawdown during Deep Foundation Pit Dewatering. *Water* **2021**, *13*, 3297. https://doi.org/10.3390/w13223297

Academic Editor: Aldo Fiori

Received: 2 November 2021
Accepted: 18 November 2021
Published: 21 November 2021

1. Introduction

The groundwater basin of Shanghai is a typical multi-aquifer-aquitard system (MAAS) with a phreatic aquifer (Aq01), a low-pressure artesian aquifer (Aq02), and five confined aquifers (AqI–AqV) separated by six aquitards (AdI–AdVI) from the top to the bottom [1–6]. Groundwater control is essential for the foundation pit construction in Shanghai to avoid the risk of pit bottom gushing and flowing sand that resulted from the confined aquifer rich of groundwater [7–11]. Foundation pit dewatering with the combination of a waterproof curtain and pumping wells (wall-well) is generally used to ensure the stability of the foundation pit bottom [12–15]. Theoretically, the use of a full-penetrating waterproof curtain can block the groundwater connection between the inside and outside of the foundation pit, which can effectively reduce the groundwater drawdown and ground settlement outside the pit [16–19]. However, compared with a fully cut-off waterproof curtain, the partial penetrating waterproof curtain is adopted widely during the construction of the foundation pit due to the constraints of construction technology, cost, or the surrounding environment [20]. The partial penetrating waterproof curtain results in the larger groundwater drawdown and ground settlement outside the foundation pit comparing with the full-penetrating waterproof curtain [17,21,22]. Many researchers have considered the combined effect of a penetrating waterproof curtain and pumping wells (labeled as the wall-well effect) on

the surrounding environment in the foundation pit dewatering during the shallow-middle underground space development [23–25].

During the development of shallow-middle underground space in Shanghai, the confined aquifer layers related to the foundation pit construction mainly include Aq02 and AqI [26]. In recent years, the scale and depth of underground space utilization is increasing in Shanghai with the urbanization, and the excavation depth of the foundation pit has reached 30–50 m and even 60 m [27,28]. With the deepening of the foundation pit excavation, some ultra-deep foundation pits have been involved in deep confined aquifers including AqII and even AqIII [29]. AqII of Shanghai is generally buried at 60–70 m in depth with a thickness of 20–30 m [30,31]. There is a hydraulic connection between AqII and the underlain AqIII in some scattered areas, thus forming an aquifer with a thickness of over 50 m, of which the groundwater is rich and the permeability coefficient is large. Since the characteristics of AqII and AqIII are different from those of Aq02 and AqI, the feasibility of the existing research results of the wall-well effect on the surrounding environment, which are obtained during the shallow-middle underground space development, should be further verified on the deep foundation pit. Moreover, the existing research has paid much attention to the impact on the buried depth of the waterproof curtain. However, simply increasing the buried depth of the waterproof curtain is not easy to achieve in the deep foundation pit [32]. The pumping well also plays an important role in the evaluation of the wall-well effect [33]. The length and the buried position of the filter tube of the pumping well, which are the key issues in the design of the pumping well, will affect the seepage path of groundwater directly. There are few studies on the design of the filter tube in AqII, and only little research mentioned that the shorter filter tube has a better alleviating impact of the environmental effect outside the deep foundation pit, but the result should be further verified by more engineering cases [34].

The aim of this paper is to integrate the theoretical basis for the design of a filter tube in foundation pit dewatering and give suggestions for the wall-well setting in engineering practice, especially in deep aquifers of Shanghai. The impact of the filter tube of the pumping well on the groundwater drawdown outside the pit is investigated by a numerical simulation model. An ultra-deep foundation pit that involved deep aquifers in Shanghai is taken as an example. Firstly, the project background description is introduced. Secondly, the numerical model is established and modified by a pumping test. Then, the impact of the position and length of the filter tube on the groundwater drawdown difference between outside and inside the pit are analyzed, respectively. Finally, suggested and optimal values for the design of a filter tube in a deep foundation pit dewatering project are proposed.

2. Project Background Description

2.1. Project Overview

Figure 1 shows the plan view of foundation pit. The foundation pit is similar to rectangular, of which the length ranges from 71.8 to 75.3 m and the width is 22 m. The pit is divided into two areas, namely the north part with an excavation depth (D_e) of 36.92 m (negative value means below ground surface) and the south part with a D_e of 39.80 m. The pit has two rings of waterproof curtains with an interval of about 6.5 m. A diaphragm wall with a thickness of 1.2 m and a buried depth (D_{iw}) of 83 m is set as the inner waterproof curtain (labeled as the inner-wall) and a cement soil mixing wall with a buried depth (D_{ow}) of 60.3 m is set as the outer waterproof curtain (labeled as the outer-wall).

2.2. Engineering Geological and Hydrogeological Conditions

The soil layers in the project site are divided into 13 layers from the top to the bottom according to the geologic origin, soil structure, and characteristics, including artificial soils (labeled as 1_1), silty clay (2), mucky clay with clayey silt (3), mucky clay (4), clay (5_1), silty clay (5_3), silty clay (5_4), clay (6), sandy silt (7_1), silty fine sand (7_2), silty clay with silt sand (8_{21}), silty fine sand (9), and silty fine sand (11). The soil profile and properties of soil layers are presented in Figure 2.

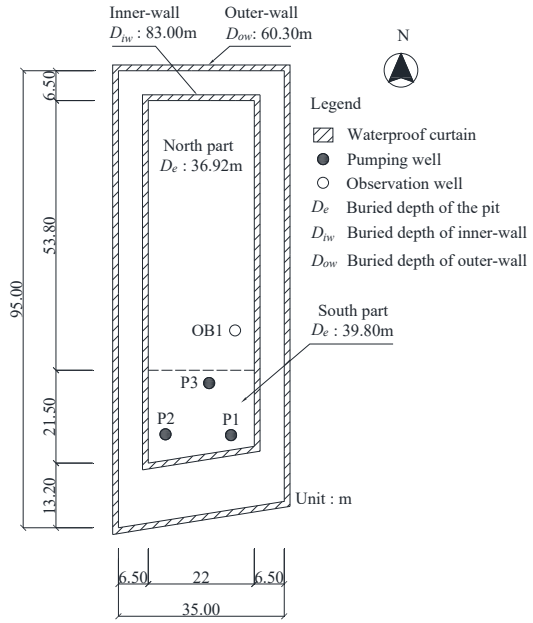

Figure 1. Plan view of foundation pit (recreated based on [35]).

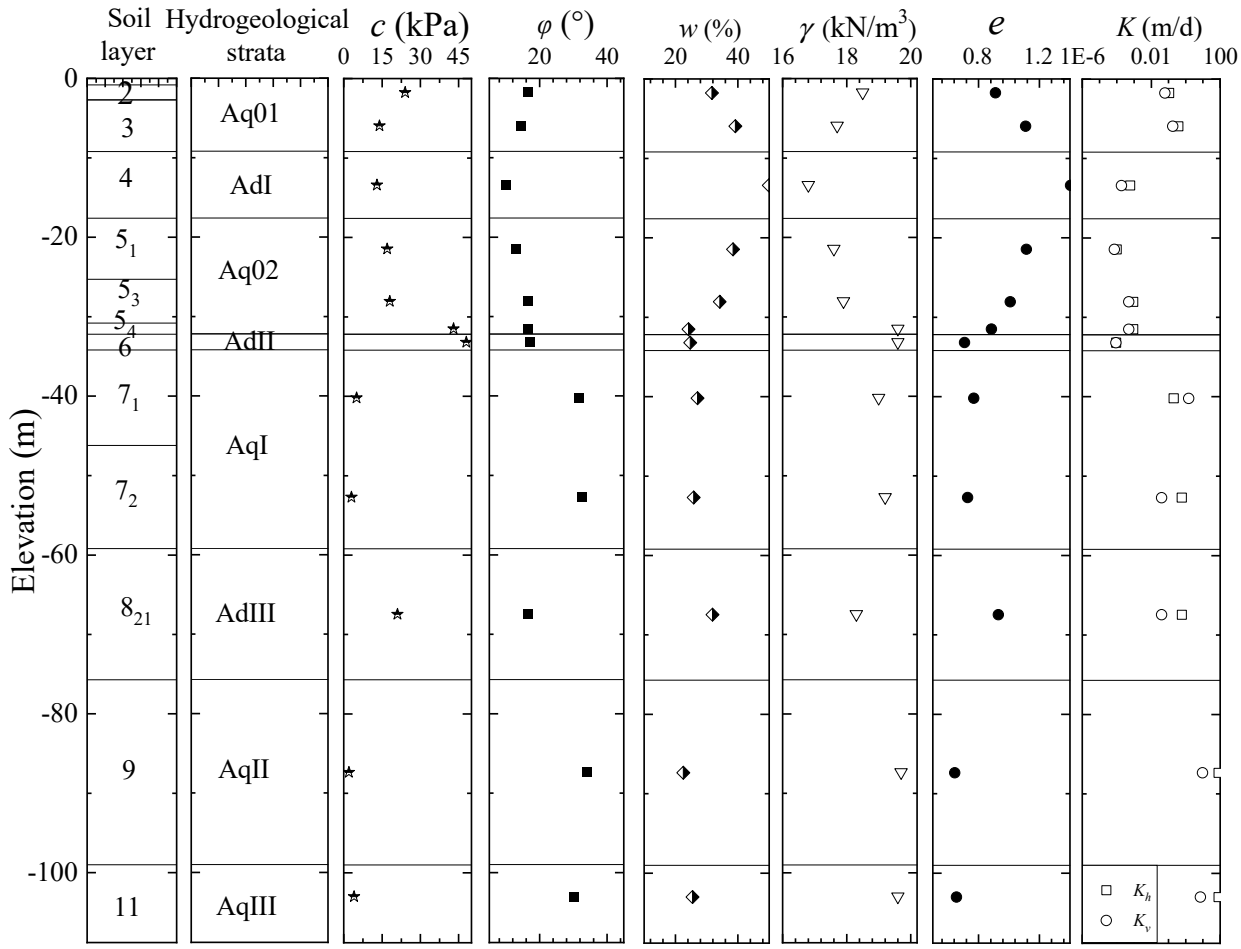

Note: c = cohesion; φ = internal friction angle; γ= unit weight; e = void ratio; w= water content; K_h , K_v= Horizontal and vertical hydraulic conductivity.

Figure 2. Soil profile and properties of soil layers.

The hydrogeology within the influenced depth of the foundation excavation includes a phreatic aquifer (Aq01), a low-pressure artesian aquifer (Aq02), and three confined aquifers (AqI–AqIII). Aq01 is contained in soil layers 1_1, 2, and 3, which is affected by rainfall, surface water, and tidal fluctuation. The groundwater level of Aq01 is −0.5 to −1.0 m (negative value indicates below the ground surface). The confined water mainly affects the excavation of the foundation pit, including Aq02, AqI, and AqII. The information of each confined aquifer is described in detail as follows:

(1) Aq02: The groundwater level is −0.50 to −3.80 m, which is contained in the soil layers 5_1, 5_3, and 5_4. The measured water inflow rate of a single well is about 1.2 m^3/h, and the K_h and K_v are 8.99×10^{-4} m/d and 4.96×10^{-4} m/d, respectively.

(2) AqI: The groundwater level is −1.40 to −2.64 m, which is contained in soil layers 7_1 and 7_2. The measured water inflow rate of a single well is about 7.9 m^3/h, and the K_h and K_v are 3.97×10^{-2} m/d and 0.59×10^{-2} m/d, respectively.

(3) AqII: The groundwater level is −4.78 to −7.04 m, which is contained in soil layer 9. The measured water inflow rate of a single well is about 212–500 m^3/h, and the K_h and K_v are 79.49 m/d and 9.50 m/d, respectively.

(4) AqIII: This layer is contained in soil layer 11 and connected with AqII directly, the groundwater level is the same as AqII. The measured water inflow rate of a single well is 273–480 m^3/h, the K_h and K_v are 48.38 m/d and 6.48 m/d, respectively.

2.3. Field Pumping Test

The bottom of the foundation pit is located in layer 7_1. In view of the deep and thick aquifer resulting from the hydraulic connection between AqII and AqIII, the dewatering measures with a partial penetrating waterproof curtain are adopted. The toe of the inner-wall is inserted into layer 9. For the stability of the deep foundation pit bottom, the groundwater drawdown of the confined aquifer underlain the pit is determined by the traditional pressure balance method [16]. In this case, the drawdown of the groundwater level of AqII should be 7.38 m before excavation of the foundation pit.

A pumping test is conducted to ensure the construction safety and evaluate the dewatering effect on the environment. For the dewatering design scheme of the pumping test in layer 9, there are three pumping wells (P1 to P3) and one observation well (OB1) inside the pit, as shown in Figure 1. The profile of all the wells is shown in Figure 3. Table 1 presents the schedule of the pumping test. The total pumping test time is 31 h, and P3 stops pumping for 6 h in the middle of the test.

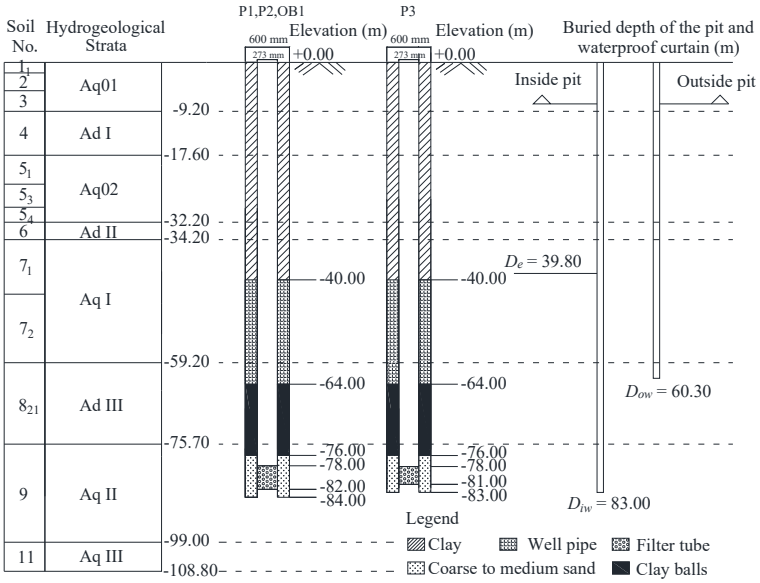

Figure 3. Profile of pumping and observation wells (recreated based on [35]).

Table 1. Schedule of the pumping test.

Pumping Well	Observation Well	Pumping Time t (d)	Discharge Rate Q (m^3/h)
P1	OB1	0–1.30	240
P2		0–1.30	266
P3		0–0.50, 0.75–1.30	160

3. Numerical Simulations

3.1. Mathematical Model and Software Introduction

In order to analyze the environmental effect outside the pit of AqII dewatering, the finite different method simulation method combined with the three-dimensional groundwater seepage model was applied [36–39]. The three-dimensional groundwater seepage mathematical model is:

$$\begin{array}{ll} \frac{\partial}{\partial x}\left(K_{xx}\frac{\partial H}{\partial x}\right)+\frac{\partial}{\partial y}\left(K_{yy}\frac{\partial H}{\partial y}\right)+\frac{\partial}{\partial z}\left(K_{zz}\frac{\partial H}{\partial z}\right)-q=S_s\frac{\partial H}{\partial t} & (x,y,z) \\ H=H_1(x,y,z,t) & (x,y,z)\in\Gamma_1 \\ H=H_2(x,y,z,t) & (x,y,z)\in\Gamma_2 \\ \frac{\partial H}{\partial n}=K_{xx}\frac{\partial H}{\partial x}\frac{\partial F}{\partial x}+K_{yy}\frac{\partial H}{\partial y}\frac{\partial F}{\partial y}+K_{zz}\frac{\partial H}{\partial z}\frac{\partial F}{\partial z}=0 & (x,y,z)\in\Gamma_3 \\ H(x,y,z,t)|_{t=t_0}=H_0(x,y,z) & (x,y,z)\in\Omega \end{array} \quad (1)$$

where K_{xx}, K_{yy}, and K_{zz} are the hydraulic conductivities along the x, y, and z directions (m/d); H is the water head; H_1 is the constant water level on Γ_1 (the first boundary at the bottom of the pit); H_2 is the constant water level on Γ_2 (the first boundary on the side of the calculated domain far from the pit); Γ_3 is the second boundary at the bottom of the calculated domain; q is the external source and sink flux (1/day); S_s is the specific storage (1/m); t is time (day); Ω is the calculated domain; n is the normal direction of the bottom of the calculated domain; and F is the surface equation of the bottom of the calculated domain.

The three-dimensional groundwater seepage model by the application of "Geoflow 3D" software is established in this study. The software can be used to simulate groundwater seepage including the water reservoir, water level, and water flow direction. This software has been widely applied for some foundation pit dewatering projects such as in Shanghai and Ningbo city [40–42]. Of course, there are some constrains in this study. The soil parameters kept steady with time, and the horizontal anisotropy of soils was not considered in the simulation process. The procedure of this software is shown in Figure 4.

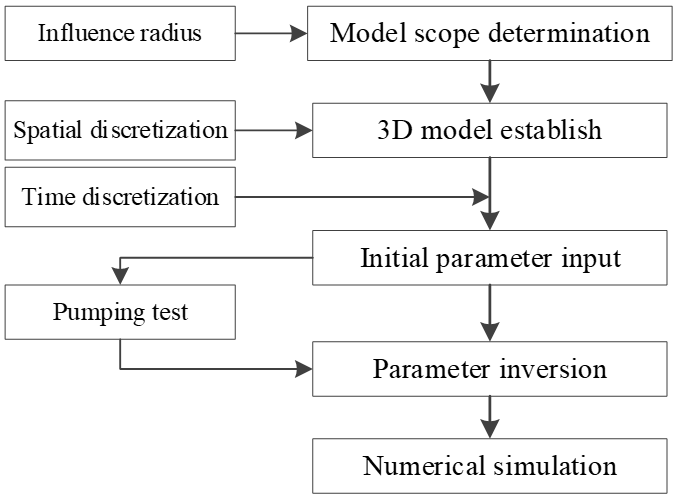

Figure 4. Flow chart of the building numerical model.

3.2. Numerical Model

Since the influence radius of the pumping test is calculated as 1500 m [35], the length and width of the numerical model are all set as 2500 m, and the depth is −108.5 m, which is equal to the buried depth at the bottom of AqIII. Figure 5 shows the three-dimensional model domain and grid mesh. The mesh size is (4–5) m × 5 m inside of the foundation pit and gradually expands to about 200 m × 200 m at the boundary. The number of nodes and elements in each plane is 1192 and 1242, respectively. Figure 6 shows the local expanded grid plane in the foundation pit. In the vertical direction, eight strata are set according to the actual hydrogeological conditions, in which the initial groundwater levels of AqI, AqII, and AqIII are −1.45 m, −5.42 m, and −5.64 m, respectively. The four lateral boundaries are set to fixed hydraulic head boundaries equal to the initial groundwater level, and the bottom boundary is set to the confining boundary. The total number of numerical model nodes and elements are 34,568 and 34,776, respectively. The positions of the pumping wells and the observation wells are set as shown in Figure 6.

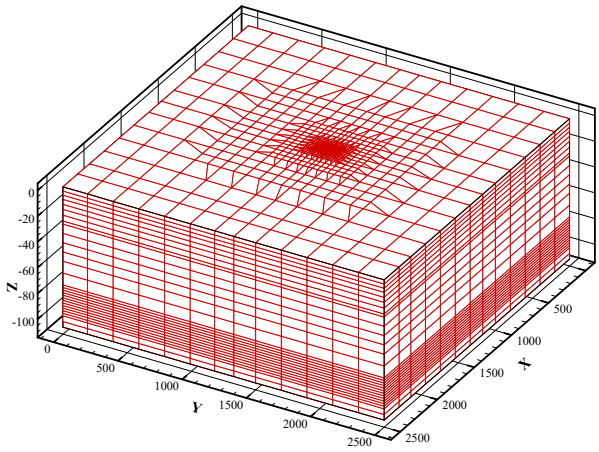

Figure 5. Three-dimensional model domain and the grid mesh.

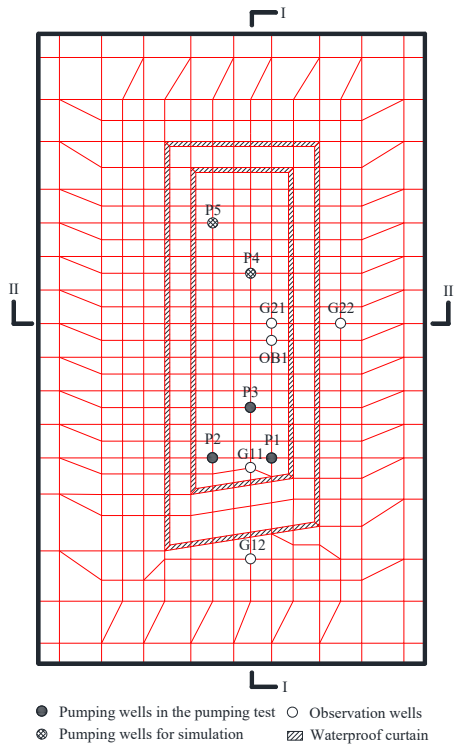

Figure 6. Plan view of local enlarged mesh inside the foundation pit.

3.3. Model Verification

Table 2 tabulates the inversed parameters in the numerical model. Figure 7 presents the comparison between measured and simulated groundwater drawdown of the observation well OB1 inside the pit under the pumping test. Due to the large volume of groundwater in layer 9 and the rapid supplement of groundwater outside the pit, the groundwater drawdown of OB1 inside the pit can meet the safety requirement of the pit bottom when P1, P2, and P3 are simultaneously pumping. The maximum groundwater drawdown of observation well OB1 is 7.36 m at 1.30 d, and the simulated data indicate 7.25 m, of which the deviation is only 1.4%. The result verifies that the simulation result is consistent with the measured data.

Table 2. Parameters used in the numerical model.

No.	Hydrogeological Strata	Thickness (m)	γ (kN/m^3)	e	K_h (m/d)	K_v (m/d)	S_S (1/m)
1	Aq01	9.60	19.00	0.651	4.32×10^{-3}	7.20×10^{-4}	1.00×10^{-4}
2	AdI	7.80	17.40	0.548	2.61×10^{-4}	1.30×10^{-4}	1.75×10^{-4}
3	Aq02	9.00	17.70	0.474	3.10×10^{-1}	1.50×10^{-1}	9.59×10^{-5}
4	AdII	2.50	19.40	0.605	1.70×10^{-2}	1.10×10^{-3}	5.47×10^{-4}
5	AqI	28.70	18.30	0.489	5.00	6.00×10^{-1}	6.38×10^{-5}
6	AdII	18.40	19.10	0.594	6.00×10^{-1}	4.00×10^{-2}	4.50×10^{-4}
7	AqII	24.00	18.70	0.405	9.50×10^{1}	9.00	2.00×10^{-5}
8	AqIII	8.80	19.10	0.470	5.50×10^{1}	7.00	3.00×10^{-5}
	Diaphragm wall				1.00×10^{-10}	1.00×10^{-10}	1.00×10^{-9}

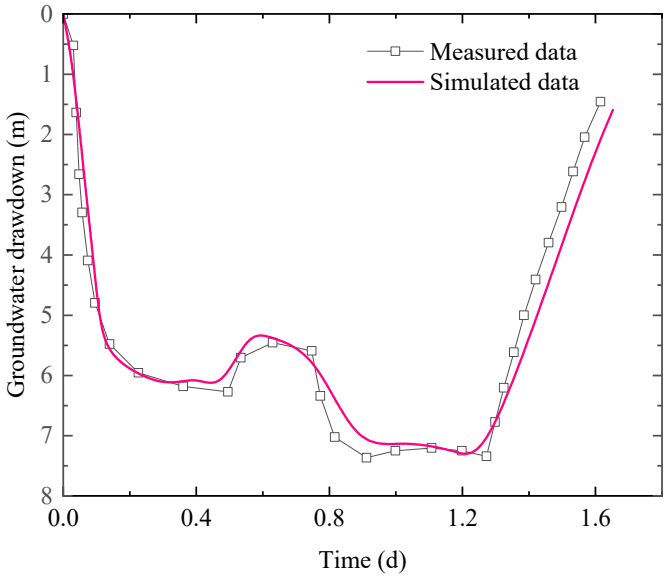

Figure 7. Comparison of measured and simulated groundwater drawdown of the observation well OB1.

4. Discussion

4.1. Wall-Well Patterns of the Dewatering Inside the Foundation Pit

Figure 8 shows the wall-well patterns of the dewatering inside the foundation pit. The relative position of the wall-well is described by R_p, which means the difference between the buried depth of the bottom of the filter tube (D_b) and that of the waterproof curtain (D_w). There are three wall-well patterns according to R_p via considering the seepage path during dewatering, namely the full-closed pattern (Pattern-I), part-closed pattern (Pattern-II), and none-closed pattern (Pattern-III). The three wall-well patterns are introduced as follows:

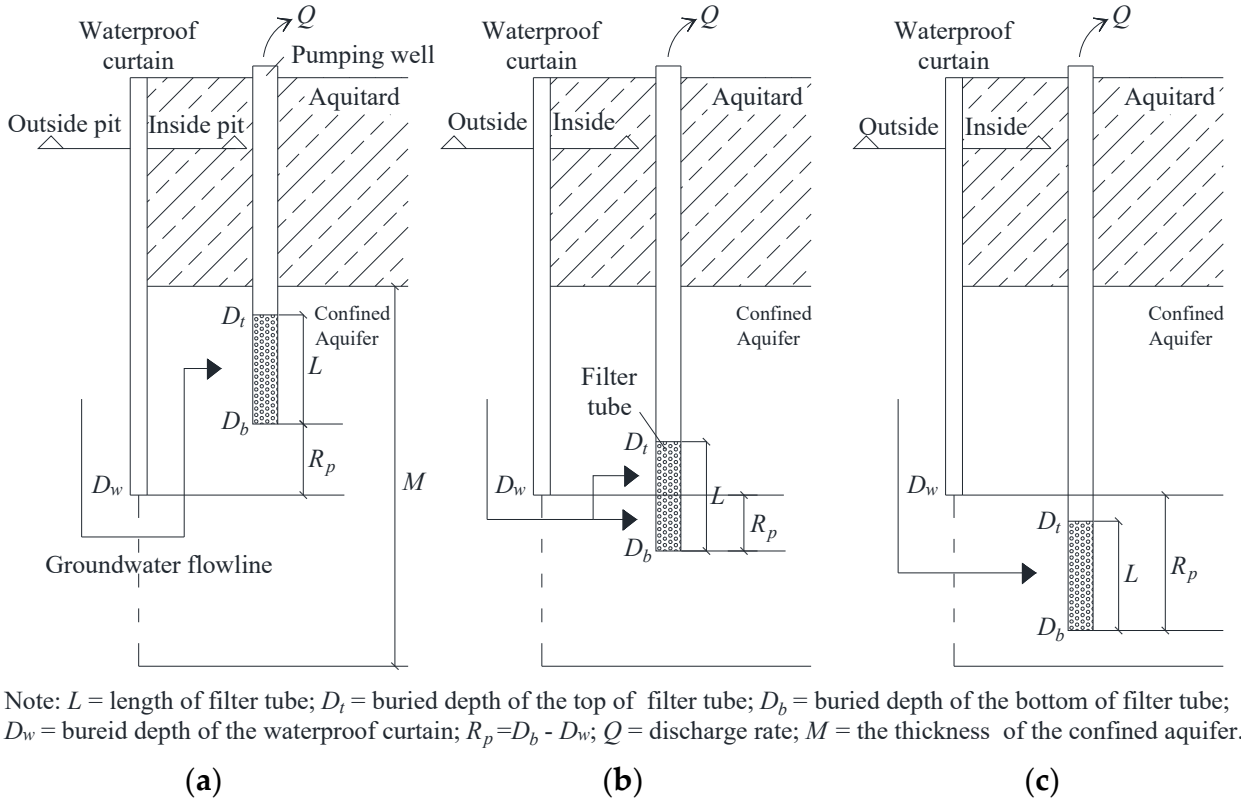

Note: L = length of filter tube; D_t = buried depth of the top of filter tube; D_b = buried depth of the bottom of filter tube; D_w = bureid depth of the waterproof curtain; R_p =D_b - D_w; Q = discharge rate; M = the thickness of the confined aquifer.

(**a**) (**b**) (**c**)

Figure 8. Wall-well patterns of the dewatering inside the foundation pit (recreated by [43,44]). (**a**) Full-closed pattern; (**b**) Part-closed pattern; (**c**) None-closed pattern.

(1) Pattern-I: As shown in Figure 8a, the whole filter tube is located above the bottom of the waterproof curtain, indicating $R_p \leq 0$. Under the action of the head difference between the outside and inside pit, the groundwater outside the pit flows over the bottom of the waterproof curtain and then into the filter tube. The groundwater seepage path of Pattern-I is the longest of the three patterns.

(2) Pattern-II: As shown in Figure 8b, part of the filter tube is located below the bottom of the waterproof curtain, indicating $0 < R_p < L$. Part of the groundwater outside the pit flows into the filter tube along the toe of the waterproof curtain. The other part flows into the filter tube over the waterproof curtain, which is similar with Pattern-I. The seepage path of part-closed pattern is shorter than that in the full-closed pattern.

(3) Pattern-III: As shown in Figure 8c, the whole filter tube is located below the bottom of the waterproof curtain, indicating $R_p \geq L$. Groundwater flows into the filter tube along the toe of the waterproof curtain. The seepage path of Pattern-III is the shortest of the three patterns.

4.2. Simulation Cases and Results Considering Wall-Well Patterns

For the convenience to discuss the impact of wall-well patterns on the groundwater drawdown, D_{iw} is changed to a constant value of 92 m in the subsequent numerical simulation. Since the pumping wells and observation wells of the pumping test are only concentrated in the south part of the pit, the dewatering effect of the north pit is not investigated yet. Therefore, two pumping wells for numerical simulation (P4 and P5) are added to the north part, as shown in Figure 6. G11, G12, G21, and G22, which are also shown in Figure 6, are added as observation wells for the groundwater level.

The filter tube of the pumping wells is designed in two conditions as follows: (1) Condition I: this condition changes R_p. The L of all the pumping wells (P1 to P5) is constant as 4 m, and R_p varies from −12 to 8 m with an increment of 2 m.; (2) Condition II: this condition changes L. The top of the filter tube is set to the top surface of AqII, which means D_t is

equal to 76 m, and L varies from 4 to 24 m with an increment of 2 m. R_l equal to L divided by the thickness of the dewatering aquifer M is used to evaluate the incompleteness of the pumping wells. The corresponding R_l changes from 16.7% to 100% in this condition. There are 11 calculation cases in each condition, which are listed in Table 3.

Table 3. Simulated cases considering different R_p and L values.

Condition I (L = 4 m)					Condition II (D_t = 76 m)					
Pattern	**Calculation Case**	R_p **(m)**	D_t **(m)**	D_b **(m)**	**Pattern**	**Calculation Case**	L **(m)**	R_l **(%)**	R_p **(m)**	D_b **(m)**
I	I−1	−12	76	80	I	II−1	4	16.7	−12	80
	I−2	−10	78	82		II−2	6	25.0	−10	82
	I−3	−8	80	84		II−3	8	33.3	−8	84
	I−4	−6	82	86		II−4	10	41.7	−6	86
	I−5	−4	84	88		II−5	12	50.0	−4	88
	I−6	−2	86	90		II−6	14	58.3	−2	90
	I−7	0	88	92		II−7	16	66.7	0	92
II	I−8	2	90	94	II	II−8	18	75.0	2	94
III	I−9	4	92	96		II−9	20	83.3	4	96
	I−10	6	94	98		II−10	22	91.7	6	98
	I−11	8	96	100		II−11	24	100	8	100

Figure 9 shows the numerical results of partial calculation cases. Under the condition of constant groundwater drawdown inside the pit, the environmental effect of foundation pit dewatering is obviously different when the design parameters regarding the filter tube of the pumping well changed. For Condition I, the groundwater drawdown outside the pit increases with the increase of R_p. The maximum groundwater drawdown outside the pit increased from 2.23 m when R_p is −12 m to 6.40 m when R_p is 8 m. For Condition II, the groundwater drawdown outside the pit increases with the increase of R_l. The maximum groundwater drawdown outside the pit increased from 2.14 m when R_l is 16.7% to 2.98 m when R_l is 100%.

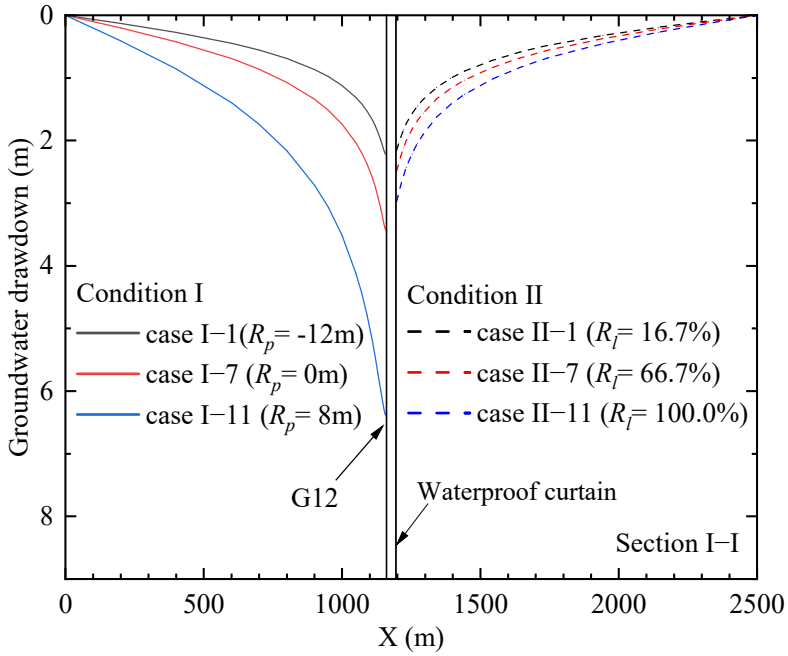

Figure 9. Groundwater drawdown outside the pit under different calculation cases on section I-I.

Figure 10 shows the groundwater drawdown on both sides of the waterproof curtain. G11 and G12, G21, and G22 are two groups of observation points for the groundwater level on both sides of the waterproof curtain, the former of which is inside the pit with a distance to the waterproof curtain of 4 m, and the latter is outside the pit with a distance to the waterproof curtain of 5 m. With the increase of R_p and R_l, the groundwater drawdown of G11, G21 inside and G21, G22 outside the pit both shows an increasing trend. It should be noted that the variations of groundwater drawdown inside the pit are small, while those outside the pit are large. Especially the variations of groundwater drawdown outside the pit in Condition I are much larger than those in Condition II. So, the impact on the groundwater drawdown by R_p is greater than that by R_l.

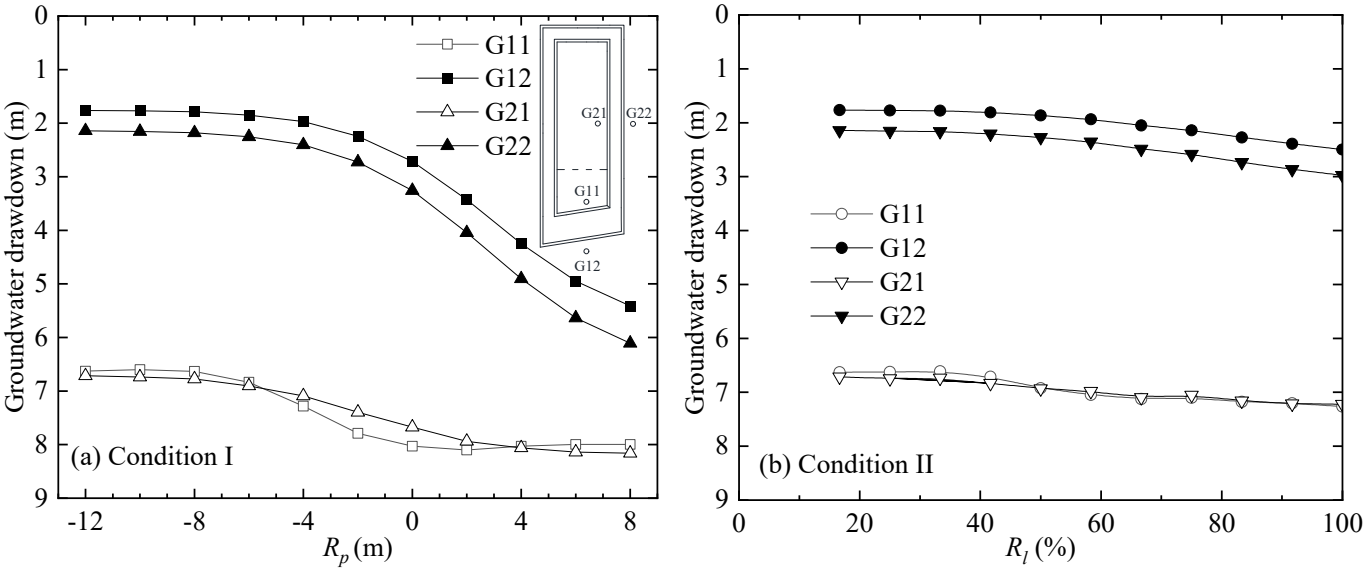

Figure 10. Groundwater drawdown on two sides of the waterproof curtain in different calculation cases: (**a**) Condition I; (**b**) Condition II.

Under the action of groundwater drawdown difference between inside and outside the pit, groundwater flows over the curtain to the filter tube of the pumping well. On the condition of a constant value M and D_w, the seepage area and seepage path mainly vary with the design of the pumping well [45], including R_p and R_l. So, the groundwater drawdown difference between G11 (G21) and G12 (G22) (labeled as Δh) is applied for further analysis on the impact of R_p and R_l on the change of groundwater level.

4.3. Impact of the Position of Filter Tube

Figure 11 shows the relationship between Δh and R_p in Condition I. In general, Δh first increases and then decreases with the increase of R_p, but the change rate of Δh presents a major difference. According to the wall-well patterns shown in Figure 8, the $R_p-\Delta h$ plot can be divided into three parts as follows: (1) Pattern-I (-12 m $< R_p \leq 0$ m): the whole filter tube is located above the bottom of the waterproof curtain at this part, Δh increases first and then decreases with the increase of R_p. At this stage, Δh reaches the maximum value when R_p is about -2 m; (2) Pattern-II (0 m $< R_p <$ 4 m): a partial filter tube is located below the bottom of the waterproof curtain at this part. Δh keeps decreasing with the increase of R_p. Since $D_b > D_w$, the groundwater seepage path from outside the pit to the filter tube becomes shorter than Pattern-I, leading to the supplement of groundwater outside the pit to inside the pit accelerating; (3) Pattern-III (4 m $\leq R_p <$ 8 m): the whole filter tube is located below the bottom of the waterproof curtain at this part. Δh keeps decreasing with the increase of R_p and drops to the minimum value gradually. Since the waterproof curtain cannot act as a barrier effectively [46], the supplement of groundwater outside the pit to inside the pit is the strongest compared with Pattern-I and Pattern-II.

The impact on Δh in Pattern-III is the greatest of the three patterns. Just considering the value of Δh, Pattern-III is not suggested for adoption in field engineering, because Pattern-I and Pattern-II could both meet the requirements of groundwater drawdown, as shown in Figure 11. Under the requirement of a certain value of Δh, R_p in Pattern-II is much larger than that in Pattern-I. Therefore, Pattern-I is better than Pattern-II just by the economic consideration.

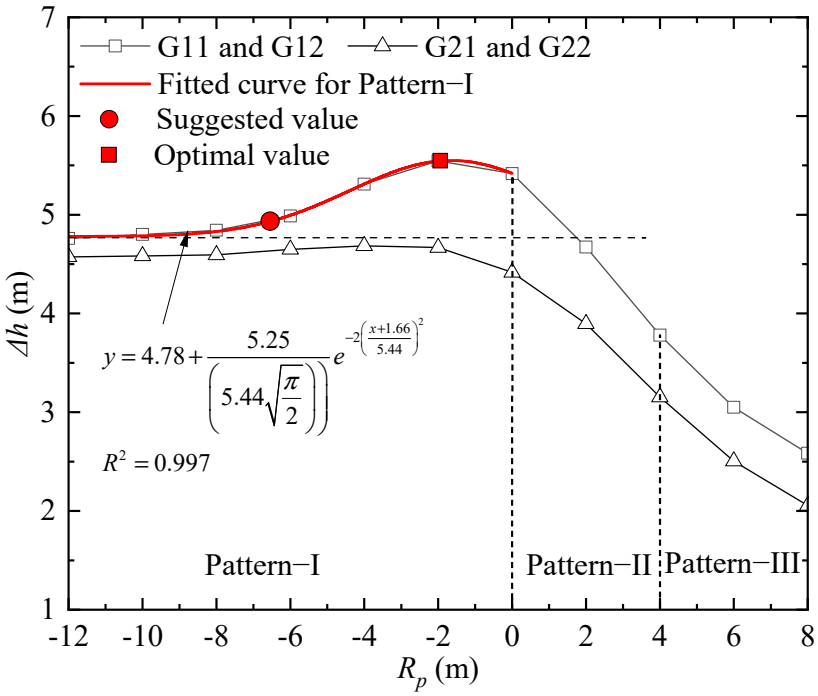

Figure 11. Relationship between R_p and Δh.

The curve of Pattern-I can be fitted by a Gaussian function. The maximum and minimum points of the second derivative of the fitted function are defined as the suggested value and the optimal value of R_p in Pattern-I respectively. When R_p is larger than the suggested value, the increment rate of Δh increases quickly. When R_p is equal to the optimal value, the maximum Δh can be obtained. As shown in Figure 11, the suggested and the optimal value of R_p are -6.41 m and -1.92 m for Pattern-I. In the process of engineering, the suggested value or the optimal value of R_p can be obtained from numerical simulation. Although increasing D_w can also relieve the environmental effect, the optimal design on the pumping wells is more reasonable and economical than increasing D_w to reduce the environmental effects in the construction of a deep foundation pit.

4.4. Impact of the Length of Filter Tube

Figure 12 shows the relationship between R_l and Δh in Condition II. In general, Δh first increases and then decreases with the increase of R_l. According to the wall-well patterns in Figure 8, the $R_l - \Delta h$ plot can be divided into two parts: (1) Pattern-I ($16.7\% \leq R_l < 66.7\%$): Δh increases slowly and then decreases at this part, in which Δh reaches the maximum value when R_l is around 58.0%; (2) Pattern-II ($66.7\% \leq R_l \leq 100\%$): Δh keeps decreasing with the increase of R_l and drops to the minimum gradually. The wall-well effect turns to Pattern-II, and the curve in this part can be fitted by the HyperbolaGen function. With the increase of R_l, the seepage path of groundwater from the outside is shorter, while Δh decreases to the minimum gradually.

The curve in Pattern-I can be fitted by the Gaussian function. The maximum and minimum points of the second derivative of the fitted function are defined as the suggested value and the optimal value. The increment rate of Δh becomes fast when R_l exceeds the

suggested value. When R_l is equal to the optimal value, the maximum Δh can be obtained. The suggested and optimal values of R_l are 38.7% and 58.2%, respectively.

The position and length of the filter tube is controlled by factors such as the permeability coefficient of the aquifer, groundwater replenishment conditions, design requirements for groundwater drawdown, and environmental conditions around the foundation pit. Wu et al. indicated that the dewatering efficiency is controlled by the three-dimensional flow in the pumping well and the depth of the retaining structure [12]. On the ideal assumption of the numerical model in this study, Pattern-I is superior to Pattern-II. However, for deep aquifers such as AqII, the permeability coefficient and the thickness may be inhomogeneous, which is different from the assumptions of the numerical model in this study. In practice, the waterproof curtain may not reach the ideal burial depth, and Pattern-II can also be considered in field engineering. Of course, the value of D_b should avoid being much more than D_w, which means R_p should be limited.

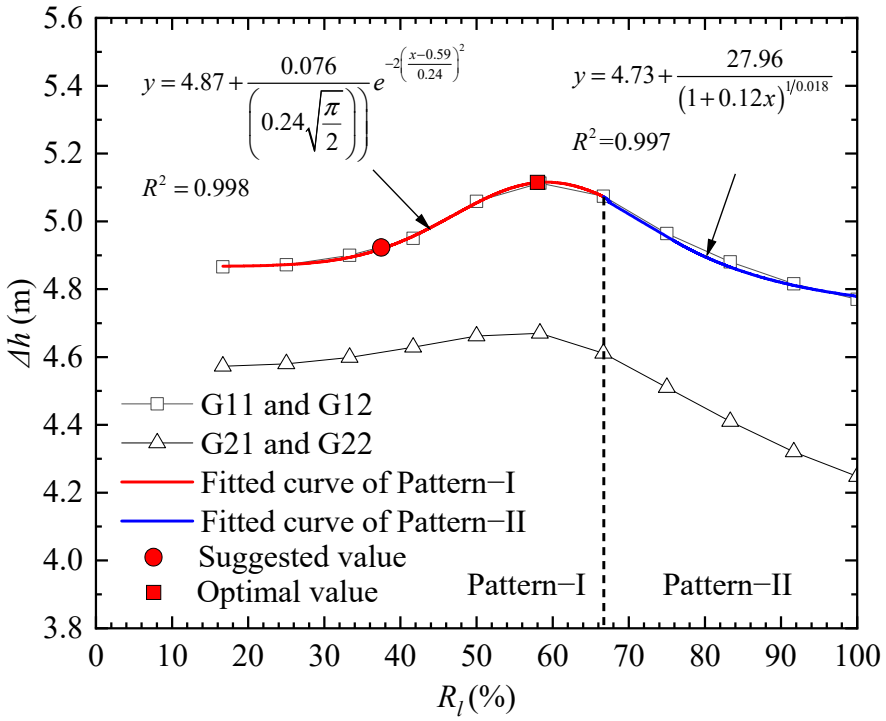

Figure 12. Relationship between R_l and Δh.

5. Conclusions

This paper investigated the impact on the groundwater drawdown outside the pit by the filter tube of the pumping well. By taking an ultra-deep foundation pit in Shanghai as an engineering case, the relationship among the parameters related to the position of the wall-well (R_p), the length of the filter tube (R_l), and the groundwater drawdown difference at both sides of the waterproof curtain (Δh) are discussed by numerical simulation. The conclusions drawn from this study are as follows:

(1) Three wall-well patterns are divided according to the relative position of the wall-well: full-closed pattern (Pattern-I), part-closed pattern (Pattern-II) and none-closed pattern (Pattern-III).

(2) The groundwater drawdown outside the pit increases with the increase of R_p and R_l, and the influence of R_p is larger than R_l.

(3) The $R_p-\Delta h$ curve shows a trend of a single-peak curve, which can be divided into three parts according to the wall-well patterns. Δh reaches the maximum value in the part of Pattern-I. The $R_p-\Delta h$ curve in Pattern-I can be fitted by the Gaussian function. The suggested and optimal values of R_p are −6.41 m and −1.92 m, respectively, according to the characteristics of the Gaussian function.

(4) The $R_l-\Delta h$ curve shows a trend of a single-peak curve, which can be divided into two parts according to the wall-well patterns. Δh reaches the maximum value in the part of Pattern-I. The $R_l-\Delta h$ curve in Pattern-I can be fitted by the Gaussian function. The suggested and optimal values of R_l are 38.7% and 58.2%, respectively.

(5) Pattern-III is not suggested in the field engineering because of its shortest seepage path within the three patterns. Pattern-II may be applied considering the complexity of actual deep foundation construction. Pattern-I is an optimal wall-well pattern on the ideal condition. The values of R_p and R_l should be between the suggested value and optimal value when Pattern-I is applied.

Author Contributions: Conceptualization, X.Z. and Y.X.; methodology, Y.X.; software, X.W.; writing—original draft preparation, X.Z.; writing—review and editing, X.Z., X.W. and Y.X. All authors have read and agreed to the published version of the manuscript.

Funding: This research was funded by the National Natural Science Foundation of China (NSFC) (Grant No. 41877213). This financial support is gratefully acknowledged.

Institutional Review Board Statement: Not applicable.

Informed Consent Statement: Not applicable.

Data Availability Statement: This study does not report any data.

Conflicts of Interest: The authors declare no conflict of interest.

References

1. Xu, Y.S.; Shen, S.L.; Du, Y.J. Geological and hydrogeological environment in Shanghai with geohazards to construction and maintenance of infrastructures. *Eng. Geol.* **2009**, *109*, 241–254. [CrossRef]
2. Xu, Y.S.; Wu, H.N.; Shen, J.S.; Zhang, N. Risk and impacts on the environment of free-phase biogas in Quaternary deposits along the coastal region of Shanghai. *Ocean Eng.* **2017**, *137*, 129–137. [CrossRef]
3. Zhou, N.Q.; Vermeer, P.A.; Lou, R.X.; Tang, Y.Q.; Jiang, S.M. Numerical simulation of deep foundation pit dewatering and optimization of controlling land subsidence. *Eng. Geol.* **2010**, *114*, 251–260. [CrossRef]
4. Wu, Y.X.; Zheng, Q.; Zhou, A.N.; Shen, S.L. Numerical evaluation of the ground response induced by dewatering in a multi-aquifer system. *Geosci. Front.* **2021**, *12*, 101209. [CrossRef]
5. Zeng, C.F.; Wang, S.; Xue, X.L.; Zheng, G.; Mei, G.X. Evolution of deep ground settlement subject to groundwater drawdown during dewatering in a multi-layered aquifer-aquitard system: Insights from numerical modelling. *J. Hydrol.* **2021**, *603*, 127078. [CrossRef]
6. Yin, Z.Y.; Karstunen, M.; Chang, C.S.; Koskinen, M.; Lojander, M. Modeling time-dependent behavior of soft sensitive clay. *J. Geotech. Geoenviron. Eng.* **2011**, *137*, 1103–1113. [CrossRef]
7. Xu, Y.S.; Shen, J.S.; Zhou, A.N.; Arulrajah, A. Geological and hydrogeological environment with geohazards during underground construction in Hangzhou: A review. *Arab. J. Geosci.* **2018**, *11*, 544. [CrossRef]
8. Zeng, C.F.; Xue, X.L.; Zheng, G.; Xue, T.Y.; Mei, G.X. Responses of retaining wall and surrounding ground to pre-excavation dewatering in an alternated multi-aquifer-aquitard system. *J. Hydrol.* **2018**, *559*, 609–626. [CrossRef]
9. Wu, Y.X.; Shen, S.L.; Yin, Z.Y.; Xu, Y.S. Characteristics of groundwater seepage with cut-off wall in gravel aquifer. II: Numerical analysis. *Can. Geotech. J.* **2015**, *52*, 1539–1549. [CrossRef]
10. Wu, Y.X.; Shen, S.L.; Xu, Y.S.; Yin, Z.Y. Characteristics of groundwater seepage with cut-off wall in gravel aquifer. I: Field observations. *Can. Geotech. J.* **2015**, *52*, 1526–1538. [CrossRef]
11. Shen, S.L.; Wu, H.N.; Cui, Y.J.; Yin, Z.Y. Long-term settlement behaviour of metro tunnels in the soft deposits of Shanghai. *Tunn. Undergr. Space Technol.* **2014**, *40*, 309–323. [CrossRef]
12. Wu, Y.X.; Shen, S.L.; Yuan, D.J. Characteristics of dewatering induced drawdown curve under blocking effect of retaining wall in aquifer. *J. Hydrol.* **2016**, *539*, 554–566. [CrossRef]
13. Zeng, C.F.; Zheng, G.; Xue, X.L.; Mei, G.X. Combined recharge: A method to prevent ground settlement induced by redevelopment of recharge wells. *J. Hydrol.* **2019**, *568*, 1–11. [CrossRef]
14. Wang, J.X.; Wang, P.; Sui, D.C. Numerical simulation of pumping well-underground concrete wall-recharging well in dewatering of deep foundation pit. In *Advanced Materials Research*; Trans Tech Publication: Zurich, Switzerland, 2012; pp. 1764–1768.
15. Lu, W.; Zhao, D.; Wang, Y. The Effect of Excavation Dewatering and Supporting Structure Deformation on Soil Settlement. *Electron. J. Geotech. Eng.* **2015**, *20*, 3955–3964.
16. Wang, X.W.; Xu, Y.S. Impact of the Depth of Diaphragm Wall on the Groundwater Drawdown during Foundation Dewatering Considering Anisotropic Permeability of Aquifer. *Water* **2021**, *13*, 418. [CrossRef]

17. Xu, Y.S.; Yan, X.X.; Shen, S.L.; Zhou, A.N. Experimental investigation on the blocking of groundwater seepage from a waterproof curtain during pumped dewatering in an excavation. *Hydrogeol. J.* **2019**, *27*, 2659–2672. [CrossRef]
18. Wu, Y.X.; Shen, S.L.; Lyu, H.M.; Zhou, A.N. Analyses of leakage effect of waterproof curtain during excavation dewatering. *J. Hydrol.* **2020**, *583*, 124582. [CrossRef]
19. Li, G.M.; Li, M.S. Research on Control Measures Unclosed Curtain for Cutting off Drains on Dewatering of Foundation Pit. *Chin. J. Undergr. Space Eng.* **2020**, *16*, 921–932. (In Chinese)
20. Wu, Y.X.; Lyu, H.M.; Han, J.; Shen, S.L. Dewatering–induced building settlement around a deep excavation in soft deposit in Tianjin, China. *J. Geotech. Geoenviron. Eng.* **2019**, *145*, 05019003. [CrossRef]
21. Shi, C.H.; Sun, X.H.; Liu, S.L.; Cao, C.Y.; Liu, L.H.; Lei, M.F. Analysis of Seepage Characteristics of a Foundation Pit with Horizontal Waterproof Curtain in Highly Permeable Strata. *Water* **2021**, *13*, 1303. [CrossRef]
22. Shen, S.L.; Wu, Y.X.; Misra, A. Calculation of head difference at two sides of a cut-off barrier during excavation dewatering. *Comput. Geotech.* **2017**, *91*, 192–202. [CrossRef]
23. Yang, T.L.; Yan, X.X.; Wang, H.M.; Huang, X.L.; Zhan, G.H. Comprehensive experimental study on prevention of land subsidence caused by dewatering in deep foundation pit with hanging waterproof curtain. *Proc. Int. Assoc. Hydrol. Sci.* **2015**, *372*, 1–5. [CrossRef]
24. Wang, J.X.; Liu, X.T.; Wu, Y.B.; Liu, S.L.; Wu, L.G.; Lou, R.X.; Lu, J.S.; Yin, Y. Field experiment and numerical simulation of coupling non-Darcy flow caused by curtain and pumping well in foundation pit dewatering. *J. Hydrol.* **2017**, *549*, 277–293. [CrossRef]
25. Wang, J.X.; Liu, X.T.; Liu, S.L.; Zhu, Y.F.; Pan, W.Q.; Zhou, J. Physical model test of transparent soil on coupling effect of cut-off wall and pumping wells during foundation pit dewatering. *Acta Geotech.* **2019**, *14*, 141–162. [CrossRef]
26. Ma, L.; Xu, Y.S.; Shen, S.L.; Sun, W.J. Evaluation of the hydraulic conductivity of aquifers with piles. *Hydrogeol. J.* **2014**, *22*, 371–382. [CrossRef]
27. Li, H.Q.; Fan, Y.Q.; Yu, M.J. Deep Shanghai project–a strategy of infrastructure integration for megacities. *Tunn. Undergr. Space Technol.* **2018**, *81*, 547–567. [CrossRef]
28. Xu, Y.S.; Ma, L.; Du, Y.J.; Shen, S.L. Analysis of urbanisation induced land subsidence in Shanghai. *Nat. Hazards* **2012**, *63*, 1255–1267. [CrossRef]
29. Jia, J.; Zhai, J.Q.; Li, M.G.; Zhang, L.L.; Xie, X.L. Performance of large-diameter circular diaphragm walls in a deep excavation: Case study of Shanghai Tower. *J. Aerosp. Eng.* **2019**, *32*, 04019078. [CrossRef]
30. Shen, C. Comprehensive Control Analysis of Second Confined Aquifer of Super Deep Foundation Pit in Shanghai. *Build. Constr.* **2021**, *43*, 176–178. (In Chinese)
31. Zhang, X.S.; Wang, J.X.; Wong, H.; Leo, C.J.; Liu, Q.J.; Tang, Y.Q.; Yan, X.L.; Sun, W.H.; Huang, Z.Q.; Hao, X.H. Land subsidence caused by internal soil erosion owing to pumping confined aquifer groundwater during the deep foundation construction in Shanghai. *Nat. Hazards* **2013**, *69*, 473–489. [CrossRef]
32. Xu, Y.S.; Shen, S.L.; Du, Y.J.; Chai, J.C.; Horpibulsuk, S. Modelling the cutoff behavior of underground structure in multi-aquifer-aquitard groundwater system. *Nat. Hazards* **2013**, *66*, 731–748. [CrossRef]
33. Wu, Y.X.; Shen, S.L.; Wu, H.N.; Xu, Y.S.; Yin, Z.Y.; Sun, W.J. Environmental protection using dewatering technology in a deep confined aquifer beneath a shallow aquifer. *Eng. Geol.* **2015**, *196*, 59–70. [CrossRef]
34. Cui, Y.G. Experimental Study on Short Filter Tube Relief Well for Confined Water in the 9th Layer of Shanghai. *Build. Constr.* **2021**, *43*, 162–165. (In Chinese)
35. Yang, Z.H.; Sun, J.J. Enclosure Design and Engineering Practice of Ultra-deep Underground Working Well in Shanghai (I). *Tunn. Rail Transit* (In Chinese). **2019**, *s2*, 27–37.
36. Zhang, D.D.; Song, C.Y.; Chen, L.Z. Numerical evaluation of land subsidence induced by dewatering in deep foundation pit. *J. Shanghai Jiaotong Univ. (Science)* **2013**, *18*, 278–283. [CrossRef]
37. Pujades, E.; De Simone, S.; Carrera, J.; Vázquez-Suñé, E.; Jurado, A. Settlements around pumping wells: Analysis of influential factors and a simple calculation procedure. *J. Hydrol.* **2017**, *548*, 225–236. [CrossRef]
38. Wu, H.N.; Shen, S.L.; Chen, R.P.; Zhou, A.N. Three-dimensional numerical modelling on localised leakage in segmental lining of shield tunnels. *Comput. Geotech.* **2020**, *122*, 103549. [CrossRef]
39. Wu, Q.; Liu, Y.Z.; Luo, L.H.; Liu, S.Q.; Sun, W.J.; Zeng, Y.F. Quantitative evaluation and prediction of water inrush vulnerability from aquifers overlying coal seams in Donghuantuo Coal Mine, China. *Environ. Earth Sci.* **2015**, *74*, 1429–1437. [CrossRef]
40. Xu, Y.S.; Ma, L.; Shen, S.L.; Sun, W.J. Evaluation of land subsidence by considering underground structures that penetrate the aquifers of Shanghai, China. *Hydrogeol. J.* **2012**, *20*, 1623–1634. [CrossRef]
41. Wang, X.W.; Yang, T.L.; Xu, Y.S.; Shen, S.L. Evaluation of optimized depth of waterproof curtain to mitigate negative impacts during dewatering. *J. Hydrol.* **2019**, *577*, 123969. [CrossRef]
42. Shen, S.L.; Xu, Y.S. Numerical evaluation of land subsidence induced by groundwater pumping in Shanghai. *Can. Geotech. J.* **2011**, *48*, 1378–1392. [CrossRef]
43. Wang, J.X.; Guo, T.P.; Wu, L.G.; Zhu, Q.F.; Tang, Y.Q.; Yang, P. Mechanism and Application of Interaction Between Underground Wall and Well in Dewatering for Deep Excavation. *Chin. J. Undergr. Space Eng.* **2010**, *6*, 564–570. (In Chinese)

44. Xu, Y.S.; Wu, H.N.; Wang, B.Z.F.; Yang, T.L. Dewatering induced subsidence during excavation in a Shanghai soft deposit. *Environ. Earth Sci.* **2017**, *76*, 351. [CrossRef]
45. Finno, R.J.; Blackburn, J.T.; Roboski, J.F. Three-Dimensional Effects for Supported Excavations in Clay. *J. Geotech. Geoenviron. Eng.* **2007**, *133*, 30–36. [CrossRef]
46. Xu, Y.S.; Shen, S.L.; Ma, L.; Sun, W.J.; Yin, Z.Y. Evaluation of the blocking effect of retaining walls on groundwater seepage in aquifers with different insertion depths. *Eng. Geol.* **2014**, *183*, 254–264. [CrossRef]